# Structured and viscous water in subnanometer gaps

Tai-De Li, Jianping Gao, Robert Szoszkiewicz, Uzi Landman,* and Elisa Riedo†
*School of Physics, Georgia Institute of Technology, Atlanta, Georgia 30332, USA*
(Received 18 October 2006; published 15 March 2007)

Direct and simultaneous measurements of the normal and lateral forces encountered by a nanosize spherical silicon tip approaching a solid surface in purified water are reported. For tip-surface distances, $0\pm0.03$ nm $<d<2$ nm, experiments and grand canonical molecular-dynamics simulations find oscillatory solvation forces for hydrophilic surfaces, mica and glass, and less pronounced oscillations for a hydrophobic surface, graphite. The simulations reveal layering of the confined water density and the development of hexagonal order in layers proximal to a quartz surface. For subnanometer hydrophilic confinement, the lateral force measurements show orders of magnitude increase of the viscosity with respect to bulk water, agreeing with a simulated sharp decrease in the diffusion constant. No viscosity increase is observed for hydrophobic surfaces.

DOI: 10.1103/PhysRevB.75.115415 PACS number(s): 68.08.−p, 61.46.−w, 62.10.+s, 66.20.+d

## I. INTRODUCTION

Water under nanoconfinement is ubiquitous, with examples including clay swelling, aquaporines, ion channels,[1,2] and water menisci in microelectrical-mechanical systems.[3,4] However, the structural and rheological characteristics of nanoconfined pure[5–10] and ionized water[11–13] continue to be the subject of discussion and debate. In particular, for nanoconfined pure water, contradictory results have been reported about the presence,[14] or absence,[7,15,16] of oscillations in the solvation forces, and concerning the magnitude of the viscosity.[7,8,10,16,17] This unsatisfactory situation is mainly due to the lack of direct, high-resolution measurements of the solvation forces and viscosity for water confinements smaller than 1–2 nm. Moreover, the influence of the wettability and roughness of the confining surfaces on the properties of nanoconfined pure water remains largely unknown. On the theoretical front, past molecular-dynamics (MD) simulations of confined water employed a canonical ensemble rather than a grand canonical molecular-dynamics (GCMD) one,[18] where in the latter the confined water region is in equilibrium with a surrounding bulk water reservoir.

Here, we report on direct high-resolution atomic force microscope (AFM) measurements of oscillatory solvation forces and markedly increased viscosity in subnanometer pure water films, correlating with GCMD simulated forces, density layering, and strongly diminished diffusion. The role of wettability and roughness of the confining surfaces is also investigated. In our AFM experiments,[4,19] a nanosize spherical silicon tip is brought quasistatically to the vicinity of a flat solid surface, all immersed in purified water, while small lateral oscillations are applied to the cantilever support[20] (see Fig. 1). The normal and lateral forces acting on the tip are measured directly and simultaneously as a function of the water film thickness, i.e., tip-sample distance.[19,20] Because of the mechanical stability of our apparatus and a judicious proper choice of the cantilever stiffness,[20] we are able to measure, during force acquisition, the tip-surface distance with subangstrom resolution, all the way down to the last adsorbed water layer. In order to investigate the role of roughness and surface chemistry of the confining surfaces, we have studied water films nanoconfined between a silicon tip and three different solid surfaces: an atomically smooth hydrophilic, i.e., wetting, surface (mica), a nanorough [root-mean-squared (rms) roughness less than 1 nm] hydrophilic surface (soda lime untreated glass[4]), and an atomically smooth hydrophobic, i.e., nonwetting, surface [highly oriented pyrolytic graphite (HOPG)]. We remark that the surface of our Si tip is likely to be oxidized.[21]

## II. MATERIALS AND METHODS

The experiments were performed with a Molecular Imaging PicoPlus AFM. We remark that our direct and quasistatic normal force measurements require a signal-to-noise ratio close to the instrumental limit of an AFM working in liquids. For good protection against external mechanical vibrations, our AFM is closed in a noise-isolated box and hung up by four bungy cords with low resonance frequency. The complete system is mounted on an optical table (RS1000-36-18) from Newport. Another instrumental problem in quasistatic force measurements is that, during the tip-sample approach, the tip snaps into contact with the surface at a distance where the gradient of the tip-sample forces exceeds the cantilever

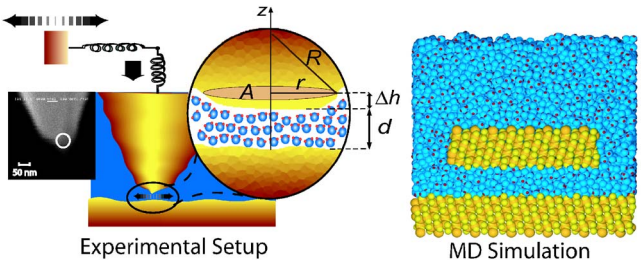


FIG. 1. (Color online) Left: an AFM was used to measure the normal and lateral forces between a nanosize untreated silicon tip and three different flat solid surfaces in de-ionized water. In this figure we also show a scanning electron microscopy (SEM) image of the tip apex. Right: an atomic configuration illustrating the MD simulation model. The water (oxygen in blue and hydrogen in red) and the quartz substrate (oxygen in yellow and silicon in dark yellow) are extended with the use of periodic boundary conditions in the *x*-*y* plane (normal to the page). The tip is fully immersed in water.

 

normal spring constant, $k_N$,[7,15] i.e., when $|\partial F_N/\partial d| \geq k_N$. To overcome this problem, we used relatively stiff cantilevers.[20]

While the AFM tip approached the solid surface in water, lateral oscillations were applied to the cantilever holder by means of a lock-in amplifier.[20] In order to shear parallel to the sample surface, before each measurement we tilted the stage that holds the sample until the difference in height of the sample surface topography across an area of $1\times1$ $\mu m^2$ (as obtained from AFM sample topography imaging) was smaller than 1 nm. This corresponds to an angle $<0.06^\circ$ between the sample surface and the tip during shearing.

We remark that even when the noise conditions were ideal, not all the measurements presented oscillations in the normal force. Oscillations were detected in seven measurements on mica, five on glass, and seven on HOPG. After scanning electron microscopy (SEM) measurements, we noted that the presence of protuberances on the tips was the origin of the disappearance of oscillations close to the solid surface. However, the results for the viscosity are nicely repeatable in all the measurements (about 30 measurements for each surface.) We estimated that the error in the normal and lateral force was about ±0.1 and 0.05 nN, respectively. The error in the piezo-$z$-position was estimated to be ±0.3 Å.

The purity of water used in our AFM liquid cell was tested after the experiment by gas chromatography–mass spectrometry (GC-MS). GC-MS spectra of used and not previously used water samples were taken by 70SE spectrometer (VG Instruments). In both cases, the results showed that any small molecular weight (less than 700 Da), organic contaminants were present at amounts below the instrumental threshold (5 ppm).

In our constant temperature (300 K) MD simulations (see Fig. 1), we employed the widely used SPC/E (simple-point-charge/extended) water model,[22] with a large cutoff distance of 3 nm, yielding a bulk density of 1.0 $g/cm^{-3}$, a surface tension of $75.8\times10^{-3}$ N $m^{-1}$, and a diffusion constant $D=2.31\times10^{-5}$ $cm^2/s$, all in very close agreement with experiments. In simulations of water confinements by crystalline wetting ($\sim0^\circ$ contact angle) $\alpha$-quartz interfaces the top surface of the substrate and the bottom layer of the tip are fully hydroxylated[23] (for the method and interaction potential parameters, see Ref. 23). In comparative simulations of nonwetting ($\sim90^\circ$ contact angle) interfaces, the hydrogens of the hydroxyl groups and all the charges of atoms in the outermost surface layer were removed and the interaction potentials of the remaining surface oxygens with water take the bulk value.

As aforementioned, in our GCMD model,[18,24] water molecules in the confined region interact with molecules outside the confinement. When the tip-to-surface gap width is varied, the number of confined molecules changes, and it is allowed to reach equilibrium, where for a given gap width, the number of confined molecules fluctuates about a constant value. In this way, the chemical potential in the confined region equals that in the surrounding bulk and corresponds to the liquid-vapor equilibrium at 300 K.

## III. RESULTS AND DISCUSSION

Oscillatory solvation forces for subnanometer water confinement were obtained previously only from indirect dynamic measurements on a soft sample,[14] where a nanotube tip is vibrated along the approach direction with an amplitude of 3.7 nm and the forces are then extracted from the measured frequency shift through a mathematical model.[14] Earlier direct quasistatic measurements of solvation forces in purified water did not show oscillations and/or could not access confinements smaller than 2.5 nm.[7,15,16]

In Fig. 2, we present direct quasi static normal force $F_N$ measurements [(A), (A′), (a), and (b)] together with theoretically calculated $F_N$ [(a′) and (b′)] as a function of the tip-sample distance $d$ for wetting and nonwetting surfaces. Figure 2(a) shows the presence of oscillations in $F_N$ vs $d$ curves when the AFM tip approaches a (wetting) nanorough glass surface in water for $0.3<d<2$ nm. Figure 2 (A′) shows $F_N$ vs $d$ for the same glass surface for the full range of distances, e.g., $0\pm0.03<d<3$ nm; the $d=0$ location was inferred as the distance for which the slope of the curve diverges. We remark that the data for separations smaller than ~0.3 nm correspond to relatively strong interactions between the last water layer and the wetting surface.[25] Figure 2(a) shows oscillatory solvation forces for a (wetting) mica surface, which is atomically smooth. The average distance $\delta$ between adjacent steps in Figs. 2(a) and 2(b) is 0.27 and 0.22 nm, respectively. Oscillations of the normal force and values of $\delta$ close to the dimension of a water molecule indicate transitions occurring when the water film passes from $n+1$ to n layers.[18,26,27]

From the inset to Fig. 2(a) (for the mica surface), we observe that for smaller $d$ values, $\delta$ decreases from 0.37 to about 0.21 nm, in agreement with the results of x-ray reflectivity measurements.[28] A maximum of four different adjacent oscillations are observed in our experiments. Our measurements indicate the presence of layering on atomically smooth and nanorough wetting surfaces. While atomic-scale roughness obliterates liquid density oscillations of hydrocarbon chain molecules (e.g., alkanes[29]), the effect is significantly weaker for globular molecules. Small $H_2O$ molecules interact strongly with point charges of the atomically rough wetting glass surface, thus "filling the holes" and effectively smoothing the morphological inhomogeneities.

Figure 2(b) shows experimental $F_N$ vs $d$ curves for a nonwetting graphite surface. The force oscillations found for this case are less developed compared to the smooth wetting surface case [Fig. 2(a)].

The stepwise shape of the experimental normal force curves reflects the inability of the cantilever to bend following the "true" force gradient in the attractive region.[7,15] However, this problem does not affect the lateral force data (see insets in Fig. 4) because the lateral force is given by the amplitude of the cantilever's torsion.

Figures 2(a′) and 2(b′) present the solvation forces for (a′) wetting and (b′) nonwetting quartz surfaces, obtained through GCMD simulations. The agreement between the salient features of the experimental and theoretical force curves is quite remarkable, exhibiting clearly a higher propensity for solvation force oscillations in the case of wetting surfaces, as well as a decreasing value of $\delta$ as the confining gap width becomes smaller.

Figure 3 shows the density profiles normal to the confining interfaces for selected gap widths ($d=1.2$, 0.7, and

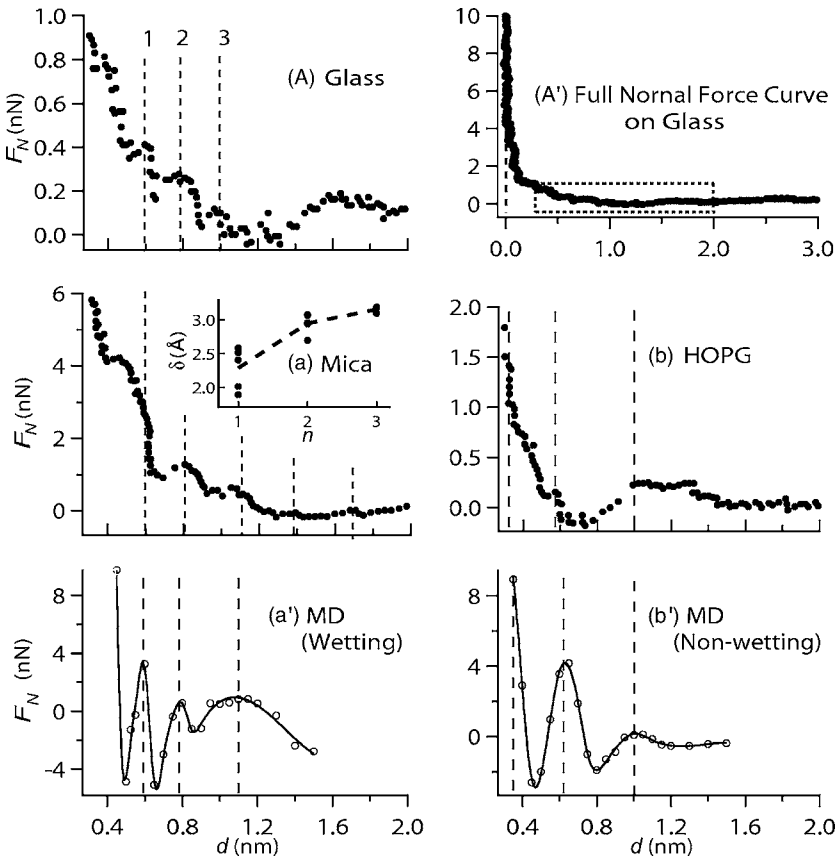


FIG. 2. $F_N$ vs $d$ for wetting [(A), (A′), (a), and (a′)] and nonwetting [(b) and (b′)] surfaces. The vertical dashed lines indicate the position of the force maxima corresponding to layer $n=1$, 2, and 3. In the inset of (a), we show values of $\delta$ corresponding to different layers, obtained from several measurements. The estimated error in $F_N$ is ±0.05 nN; the error in $d$ is ±0.3 Å.

0.5 nm) of the wetting and nonwetting confinements, as obtained from GCMD simulations. These profiles, which correlate with features in the normal force curves, illustrate the development of layering order in the water film as the degree of confinement increases. For the wetting system, the water molecules next to the confining surfaces display a double layer (DL) structure with a high peak located at about 1 Å from the surfaces and a lower peak at about 1.9 Å from the surfaces. This is due to the oxygen atoms of the hydroxyl groups on the wetting quartz surface located in four planes. The topmost one is at $z=0$ and the others are at −0.03, −0.87, and −0.90 Å. This spread (about 0.9 Å) corresponds to the width of the water DL. The DL structure occurs already at large separations between the tip and the surface and it remains up to rather narrow gaps (disappearing at about 5 Å). We have also observed hexagonal ordering for the boundary layer closest to the confining surfaces, i.e., the layer at 1 Å from the nominal surface. The molecules in the other component of the DL, i.e., at 1.9 Å from the nominal surface, are disordered. At a gap width of $d=1.2$ nm, the density profiles in the middle region are structureless and attain the experimental bulk water value. For $d=1$ nm (not shown), two density peaks separated by 3 Å develop, indicating the formation of two layers in the middle region of the confinement. These transform to a single maximum for $d=0.7$ nm [Fig. 3(b)]. When the confined water film is squeezed even further to $d=0.5$ nm, the middle layer disappears and the double peaks next to the confining surfaces merge.

The nature of the density profiles is very different for the nonwetting confining surfaces. Four broad density peaks are

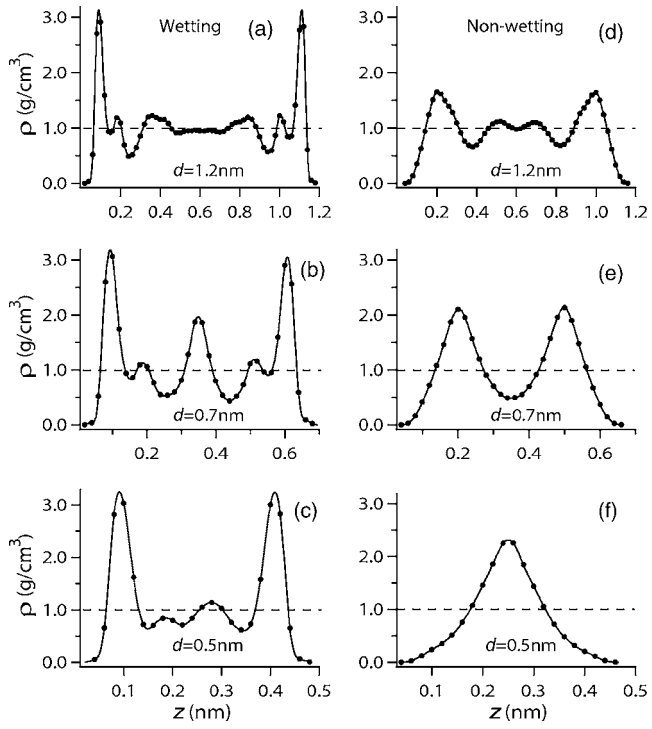


FIG. 3. MD simulated water density profiles normal to the confining interfaces, shown for selected gap widths ($d=1.2$, 0.7, and 0.5 nm) of the wetting (left) and nonwetting (right) confinements. The slight asymmetry in (c) between the two middle humps is statistical in nature.

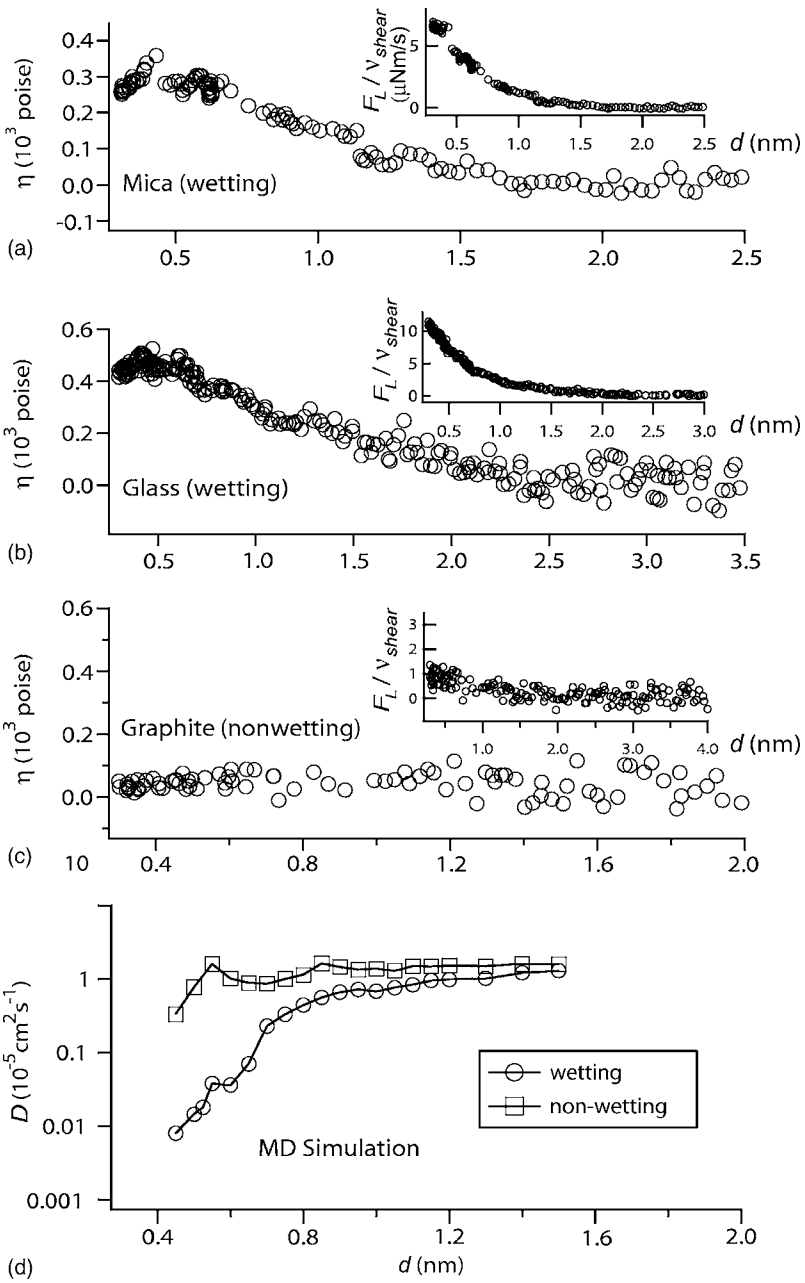


FIG. 4. Experimental $\eta$ vs $d$ as calculated from Eq. (1) (where $A=75$ nm$^2$ calculated for $\Delta h=0.25$ nm, see text) for (a) mica, (b) glass, and (c) HOPG. The estimated error in $F_L$ is $\pm 0.05$ nN; the error in $d$ is $\pm 0.3$ Å. In the insets of these figures, we show for the corresponding surfaces the experimental $F_L/v_{shear}$ vs $d$. (d) Simulated $D$ vs $d$ in water films confined by wetting and nonwetting interfaces. Only molecules remaining in the confinement during 150 ps are selected for computing the displacements. Note the nonoscillatory character of the viscosity and diffusion curves. Indeed, oscillatory variations of these quantities are found only when density layering in the gap is accompanied by the development of intralayer order (Ref. 27), which is not the case here.

seen at $d=1.2$ nm with the ones next to the confining surfaces having a higher amplitude. For $d=1$ nm, three well-defined layers develop (not shown), transforming to two well-formed peaks at $d=0.7$ nm [Fig. 3(e)]. Upon further confinement, only one peak remains [Fig. 3(f)]. The squeezing process from two to one layers corresponds to the force peaks in Figs. 2(b) and 2(b′).

To date, only a few measurements of the viscosity of confined purified water have been reported.[7,8] In the first study,[7] the surface force apparatus was used to estimate, through the use of a drainage formula, the viscosity of films with thicknesses less than 2.4 nm. In this way, a viscosity comparable with bulk water has been estimated. In the second study,[8] the viscous force in water films with thickness $d>1$ nm was derived by means of a technique based on scanning near-field optical microscopy. An increased viscosity, by up to 4 orders of magnitude, has been deduced. This is in agreement with a dramatic transition in the mechanical properties of a water meniscus found in Ref. [16,30]. Clearly, these indirect measurements yielded contradictory results and did not access the $d<1$ nm regime which is indeed the focus of our paper.

In our AFM experiments, we detect simultaneously the normal solvation forces and the viscous lateral forces as a function of the tip to sample distance. We can thus directly extract the viscosity of the water film confined between our tip and mica, glass, and HOPG surfaces [see Figs. 4(a)–4(c), respectively]. In the insets to these figures, we show the lateral force divided by the shear velocity for each surface. The viscosity has been calculated following the model of two smooth parallel sliding plates separated by a distance $d$ with a fluid in between them. The lateral force $F_L$ required to keep one plate moving at a velocity $v_{shear}$ with respect to the other one is proportional to the contact area $A$ and to $v_{shear}/d$. The

proportionality coefficient $\eta$ is called the dynamic viscosity. For a simple incompressible Newtonian fluid, $\eta$ is given by

$$\eta = \frac{F_L}{v_{shear}} \frac{d}{A}. \quad (1)$$

A more rigorous treatment of our experimental geometry involves consideration of a spherical tip of radius $R = 50$ nm, sliding close to a planar solid with a distance $d$ from the tip apex to the surface. Such a case was indeed considered by Goldman *et al.*[31] but with a constant viscosity everywhere. Since in our experiments for $d < 1.3$ nm the confined water film is able to sustain a shear stress over macroscopic times, i.e., the viscosity at $d < 1.3$ nm is much higher in the vicinity of the tip apex than everywhere else, we limit the treatment[32] to the liquid confined by the tip in a region of thickness $0 \leqslant z \leqslant d + \Delta h$ (see Fig. 1), where the solid surface is at $z = 0$. We then use the expression for the local Newtonian shear stress $\sigma = \eta[v_{shear}/(d + \Delta h(r))]$ (see Fig. 1) to evaluate the total lateral force via

$$F_L = \int_0^{r'} 2\pi r \sigma(r) dr, \quad (2)$$

where $r' = \sqrt{2R\Delta h - \Delta h^2}$. This yields the expression for the viscosity,

$$\eta = \frac{F_L}{2\pi v_{shear}\left[(R+d)\ln\left(1 + \frac{\Delta h}{d}\right) - \Delta h\right]}. \quad (3)$$

This equation gives results which are well approximated by the planar geometry considered in Eq. (1), where the effective area $A$ corresponds to the spherical segment defined by the intersection between the spherical tip and a plane at $z = d + \Delta h$. The largest difference in the viscosity calculated by using the spherical and planar approximations occurs for small $d$ and large $\Delta h$. For example, for mica with $\Delta h = 0.25$ nm (a water molecule diameter) and $d = 0.5$ nm, the spherical approximation yields $\eta = 3.5 \times 10^2$ P, while for the planar one $\eta = 3 \times 10^2$ P [see Fig. 4(a)].

For wetting surfaces [Figs. 4(a) and 4(b)], the viscosity of nanoconfined water increases when increasing the confinement, reaching a value at $d = 0.5$ nm which is 4 orders of magnitude larger than the viscosity of bulk liquid water at room temperature, i.e., about $10^{-2}$ P. The bulk viscosity of water is recovered for gaps larger than 1.6 and 2 nm for mica and glass surfaces, respectively. In contrast, for the nonwetting surface (HOPG) the viscosity of the confined water film remains constant, within experimental error, with increasing confinement [Fig. 4(c)]; the slight increase of the lateral force itself (see inset) for smaller values of the gap width is consistent with Eq. (1). These measurements are in agreement with the sharp drop in the diffusion constant $D$, [circles in Fig. 4(d)] obtained by MD calculations on the wetting surface, while $D$ remains essentially constant for the nonwetting case. We believe that the different viscosities and diffusivities between wetting and nonwetting surfaces are due to the fact that water remains well attached to wetting surfaces, while it can slip easily on nonwetting surfaces. The overall nonoscillatory (see caption of Fig. 4) increase of the viscosity and the decrease of the diffusion constant in the wetting cases originate from stronger pinning interactions between the partial charges of the water molecules and those associated with the hydrophilic surfaces as the two surfaces are brought closer to each other.

## IV. SUMMARY

We measured directly and simultaneously the normal and lateral forces encountered by a nanosize Si tip approaching a solid surface in purified water. For tip-surface distances, $0 \pm 0.03 < d < 2$ nm, we found in the experiments and the MD simulations oscillatory solvation forces for hydrophilic surfaces, mica and glass, and less pronounced oscillations for a hydrophobic, graphite, confinement. The simulations revealed layering of the confined water density and the development of hexagonal order in layers proximal to a quartz surface. For subnanometer hydrophilic confinement, we measured experimentally orders of magnitude increase of the viscosity with respect to bulk water, agreeing with a simulated sharp decrease in the diffusion constant. No viscosity increase was observed for hydrophobic surfaces.

## ACKNOWLEDGMENTS

This project was supported by NSF (DMR-0405319), ACS Petroleum Foundation, DOE (E.R.), and by the AFOSR and DOE (U.L.). The simulations were performed at the Georgia Tech Center for Computational Materials Science (CCMS) and at the DOE National Energy Research Scientific Supercomputing Center (NERSC), Berkeley, California.

*Electronic address: uzi.landman@physics.gatech.edu
†Electronic address: elisa.riedo@physics.gatech.edu

[1] O. Beckstein and M. S. P. Sansom, Phys. Biol. **1**, 42 (2004).
[2] Y. Zhou, J. H. Morais-Cabral, A. Kaufman, and R. Mackinnon, Nature (London) **414**, 43 (2001).
[3] M. Scherge, X. Li, and J. A. Schaefer, Tribol. Lett. **6**, 215 (1999).
[4] R. Szoszkiewicz and E. Riedo, Phys. Rev. Lett. **95**, 135502 (2005).
[5] J. P. Cleveland, T. E. Schaffer, and P. K. Hansma, Phys. Rev. B **52**, R8692 (1995).
[6] S. Jarvis, T. Uchhashi, T. Ishida, H. Tokumoto, and Y. Nakayama, J. Phys. Chem. B **104**, 6091 (2000).
[7] U. Raviv, P. Laurat, and J. Klein, Nature (London) **413**, 51 (2001).
[8] M. Antognozzi, A. Humphris, and M. Miles, Appl. Phys. Lett. **78**, 300 (2001).
[9] S. Jeffery, P. M. Hoffmann, J. B. Pethica, C. Ramanujan, H. O. Ozer, and A. Oral, Phys. Rev. B **70**, 054114 (2004).

[10] Y. Leng and P. T. Cummings, Phys. Rev. Lett. **94**, 026101 (2005).
[11] J. Israelachvili and R. Pashley, Nature (London) **306**, 249 (1983).
[12] Y. Zhu and S. Granick, Phys. Rev. Lett. **87**, 096104 (2001).
[13] U. Raviv and J. Klein, Science **297**, 1540 (2002).
[14] T. Uchihashi, M. Higgins, Y. Nakayama, J. Sader, and S. Jarvis, Nanotechnology **16**, S49 (2005).
[15] S. OShea and M. Welland, Appl. Phys. Lett. **60**, 2356 (1992).
[16] R. C. Major, J. E. Houston, M. J. McGrath, J. I. Siepmann, and X.-Y. Zhu, Phys. Rev. Lett. **96**, 177803 (2006).
[17] H. Kim, J. Kushmerick, J. Houston, and B. Bunker, Langmuir **19**, 9271 (2003).
[18] J. Gao, W. Luedke, and U. Landman, J. Phys. Chem. B **101**, 4013 (1997).
[19] R. Lüthi, E. Meyer, H. Haefke, L. Howald, W. Gutmannsbauer, M. Guggisberg, M. Bammerlin, and H.-J. Güntherodt, Surf. Sci. **338**, 247 (1995).
[20] We used silicon tips with radia $R=50\pm10$ nm and Ultrasharp NSC12/50 cantilevers with normal and lateral spring constants in the range of 3–4.5 and 50–120 N/m, respectively. The calibration and force detection were performed as described in Ref. 4 and 19. All the experiments were performed at 300 K in high-purity DIUF water from FisherChemicals ($p$H=6.1). The approach velocity was 0.2 nm/s. During the approach lateral oscillations parallel to the solid surface (within an angle $<0.06°$) were applied to the cantilever holder by means of a lock-in amplifier (rms speed of 8–233 $\mu$m/s, rms amplitude of 1–30 nm, and frequency of about 2 KHz). The same lock-in amplifier was then used to read the signal of the lateral force acting on the tip.
[21] K.-H. Chung, Y.-H. Lee, and D.-E. Kim, Ultramicroscopy **102**, 161 (2005).
[22] H. J. C. Berendsen, J. R. Grigera, and T. P. Straatsma, J. Phys. Chem. **91**, 6269 (1987).
[23] E. J. W. Wensink, A. C. Hoffmann, M. E. F. Apol, and H. J. C. Berendsen, Langmuir **16**, 7392 (2000).
[24] The overall size of the calculational cell (repeated periodically in the $x$-$y$ plane) is $8.25\times7.86$ nm$^2$ and it is filled with water, exposing a free surface at a height of 6.3 nm from the top layer of the quartz substrate (1.5 nm thick). The quartz tip modeled as a 1.5-nm-thick block with $x$-$y$ dimensions of $5.5\times4.9$ nm$^2$ exposing a $(1,0,-1)$ plane (approximating well the bottom of a tip with $R=50$ nm) is immersed in water, leaving a confined region whose width can be varied.
[25] P. B. Miranda, L. Xu, Y. R. Shen, and M. Salmeron, Phys. Rev. Lett. **81**, 5876 (1998).
[26] J. Israelachvili, *Intermolecular and Surface Forces* (Academic, San Diego, 1997).
[27] J. Gao, W. D. Luedtke, and U. Landman, Phys. Rev. Lett. **79**, 705 (1997).
[28] L. Cheng, P. Fenter, K. K. Nagy, M. L. Schlegel, and N. C. Sturchio, Phys. Rev. Lett. **87**, 156103 (2001).
[29] J. Gao, W. D. Luedtke, and U. Landman, Tribol. Lett. **9**, 3 (2000).
[30] After the completion of this work, a paper by Major *et al.* (Ref. 16) has been published, reporting a viscosity increase by 7 orders of magnitude for nanoconfined water. However, their work is substantially different from ours, in fact, they measure the lateral force needed to shear a water meniscus, while approaching a surface and they estimate the water viscosity from a peak observed in the lateral force. In our case, the tip and the surface are fully immersed in water and we measure the viscosity throughout the gap for width $d$ in the rangeoy $0\pm0.03<d<2$ nm.
[31] A. J. Goldman, R. G. Cox, and H. Brenner, Chem. Eng. Sci. **22**, 637 (1967).
[32] In our derivation we follow the discussion given in E. Kumacheva and J. Klein, J. Chem. Phys. **108**, 6996 (1998).